Biomedicine & Pharmacotherapy 145 (2022) 112361

Contents lists available at ScienceDirect

Biomedicine & Pharmacotherapy

journal homepage: www.elsevier.com/locate/biopha

Abnormal cannabidiol ameliorates inflammation preserving pancreatic beta cells in mouse models of experimental type 1 diabetes and beta cell damage

Isabel González-Mariscal [a,*], Macarena Pozo-Morales [a,1], Silvana Y. Romero-Zerbo [a,b,1], Vanesa Espinosa-Jimenez [a], Alejandro Escamilla-Sánchez [b], Lourdes Sánchez-Salido [c], Nadia Cobo-Vuilleumier [d], Benoit R. Gauthier [d,e], Francisco J. Bermúdez-Silva [a,e,**]

[a] Instituto de Investigación Biomédica de Málaga-IBIMA, UGC Endocrinología y Nutrición. Hospital Regional Universitario de Málaga, Universidad de Málaga, 29009 Málaga, Spain
[b] Facultad de Medicina, Departamento de Fisiología Humana, Anatomía Patológica y Educación Físico Deportiva, Universidad de Málaga, 29071 Málaga, Spain
[c] Microscopy platform, Biochemical Research Institute of Malaga (IBIMA), Malaga, Spain
[d] Andalusian Center for Molecular Biology and Regenerative Medicine (CABIMER), Seville, Spain
[e] Biomedical Research Center for Diabetes and Associated Metabolic Diseases (CIBERDEM), Madrid, Spain

ARTICLE INFO

Keywords:
Beta cell
Cannabinoids
Insulitis
Inflammation
T cells
Type 1 diabetes

ABSTRACT

The atypical cannabinoid Abn-CBD improves the inflammatory status in preclinical models of several pathologies, including autoimmune diseases. However, its potential for modulating inflammation in autoimmune type 1 diabetes (T1D) is unknown. Herein we investigate whether Abn-CBD can modulate the inflammatory response during T1D onset using a mouse model of T1D (non-obese diabetic- (NOD)-mice) and of beta cell damage (streptozotocin (STZ)-injected mice). Six-week-old female NOD mice were treated with Abn-CBD (0.1–1 mg/kg) or vehicle during 12 weeks and then euthanized. Eight-to-ten-week-old male C57Bl6/J mice were pre-treated with Abn-CBD (1 mg/kg of body weight) or vehicle for 1 week, following STZ challenge, and euthanized 1 week later. Blood, pancreas, pancreatic lymph nodes (PLNs) and T cells were collected and processed for analysis. Glycemia was also monitored. In NOD mice, treatment with Abn-CBD significantly reduced the severity of insulitis and reduced the pro-inflammatory profile of $CD4^+$ T cells compared to vehicle. Concomitantly, Abn-CBD significantly reduced islet cell apoptosis and improved glucose tolerance. In STZ-injected mice, Abn-CBD decreased circulating proinflammatory cytokines and ameliorated islet inflammation reducing intra-islet phospho-NF-κB and TXNIP. Abn-CBD significantly reduced 2 folds intra-islet $CD8^+$ T cells and reduced Th1/non-Th1 ratio in PLNs of STZ-injected mice. Islet cell apoptosis and intra-islet fibrosis were also significantly reduced in Abn-CBD pre-treated mice compared to vehicle. Altogether, Abn-CBD reduces circulating and intra-islet inflammation, preserving islets, thus delaying the progression of insulitis. Hence, Abn-CBD and related compounds emerge as new candidates to develop pharmacological strategies to treat the early stages of T1D.

1. Introduction

Glucose homeostasis is highly regulated by insulin, a hormone secreted by pancreatic beta cells necessary for the uptake, use, and storage of glucose by targeted tissues. As such, insulin is a key hormone in glucose homeostasis and, thus, its secretion is a finely regulated

Abbreviations: Abn-CBD, Abnormal cannabidiol; CBD, cannabidiol; CTL, cytotoxic T lymphocytes; i.p., intraperitoneal; NOD, non-obese diabetic; Th1, T helper type 1 cells; Th2, T helper type 2 cells; Th17, T helper type 17 cells; TXNIP, Thioredoxin-interacting protein; Treg, T regulatory cells; T1D, type 1 diabetes; T2D, type 2 diabetes; STZ, Streptozotocin.

* Corresponding author.
** Corresponding author at: Instituto de Investigación Biomédica deMálaga-IBIMA, UGC Endocrinología y Nutrición, Hospital Regional Universitariode Málaga, 29009 Málaga, Spain.
E-mail addresses: isabel.gonzalez@ibima.eu (I. González-Mariscal), javier.bermudez@ibima.eu (F.J. Bermúdez-Silva).
[1] These authors contributed equally.

https://doi.org/10.1016/j.biopha.2021.112361
Received 2 August 2021; Received in revised form 14 October 2021; Accepted 19 October 2021
Available online 3 December 2021

process within the body. Sustained hyperglycemia, due to loss of insulin secretion and/or insulin action, leads to diabetes. Insulin-dependent diabetes, known as type 1 diabetes (T1D), is an autoimmune disease that results in the progressive destruction of insulin-producing beta cells within pancreatic islets of Langerhans. Such obliteration is preceded by the infiltration of immune cells in and around islets, which constitutes a process known as insulitis [1].

Macrophages, $CD4^+$, and $CD8^+$ T cells play an important role in the development of T1D. Specific $CD4^+$ T cell subsets, including helper type 1 (Th1) and 2 (Th2), Th17, and T regulatory (Treg) cells, are involved in the adaptive immune response due to their role secreting specific sets of cytokines. Concretely, an increase in the Th1/Th2 cell ratio occurs in T1D [2], and differentiation of Naïve $CD4^+$ to Th17 cells is critical in the progression/pathogenesis of T1D [3]. Differentiation into Th1 cells is triggered by interferon gamma (IFNγ) and interleukin 12 (Il-12), whereas Th17 requires Il-6 and transforming growth factor beta (TGFβ). Both Th1 and Th17 T cells secrete pro-inflammatory cytokines (such as IFNγ, IL17, and tumor necrosis factor alpha -TNFα) that induce intra-islet inflammation, which leads to the differentiation of $CD8^+$ T cells to cytotoxic T lymphocytes (CTL). Sequentially, CTLs infiltrate the islets and induce beta cell death.

Despite the advances in our understanding of the factors involved in the pathogenesis, the prevalence of diabetes is rising, with an increase of 3% in juvenile diabetes in the last year [1]. High blood glucose due to diabetes is associated with micro- and macro-vascular complications [4], and uncontrolled hyperglycemia increases the risk of renal failure, blindness, peripheral neuropathy, and premature death [4]. Moreover, patients with T1D suffer from hypoglycemia, which is sometimes unnoticed and may have fatal consequences. To date, no prevention or cure exists for T1D, and patients require lifelong exogenous insulin injections, which do not prevent the unavoidable complications associated with an amiss glycemic control. Current therapeutic approaches aim to reduce/prevent T-cell reactivity, which is known to occur during the insulitis phase of T1D. However, the use of immunosuppressors such as anti-CD3 antibodies has failed to show durable effects alone, also showing non-islet side effects on the patient's immune system, with controversy regarding their dose-efficacy-safety [5]. Therefore, alternative approaches are urgently needed to counteract T1D [6].

Cannabinoids are known to regulate metabolism and immune action. While the roles of cannabinoids in type 2 diabetes (T2D) and obesity are fairly known [7–12], their effects on T1D have been largely unexplored. Cannabidiol (CBD) is a non-psychotropic phytocannabinoid from Cannabis sativa plant that has anti-inflammatory properties in a plethora of pathologies [13], including diabetes [14]. Abnormal cannabidiol (Abn-CBD), a non-psychotropic synthetic cannabinoid, results from the transposition of the phenolic hydroxyl group and the pentyl side chain of CBD [15]. Abn-CBD was initially described for its potent cardiovascular effects lowering blood pressure [15] and further attributed anti-tumoral [16] and glucose management properties [17,18]. In the pancreas, Abn-CBD has been reported to protect pancreatic beta cells from ER stress- and cytokine-induced apoptosis and to enhance beta cell function in cultured islets of Langerhans and insulinoma cell lines [19–21].

Here we aim to explore whether the atypical cannabinoid Abn-CBD can modulate the inflammatory response during T1D onset in mice, and its therapeutic potential for the treatment of this disease in two mouse models. Firstly, we used a genetic T1D model, the non-obese diabetic (NOD) mouse model, which develops insulitis before the onset of diabetes and in which immune cells play a strong role in the pathogenesis. Secondly, we used a pharmacological approach using a pancreatic beta cells-preferred toxin, streptozotocin (STZ), injected into healthy C57Bl/6 J mice. STZ damages beta cells, inducing loss of insulin and, hence, hyperglycemia, and a secondary response aimed at protecting beta cell mass, which includes activation of inflammatory processes and proliferation of beta cells [22]. These two animal models are complementary in terms of pathogenesis and pathophysiology, and their combined use allowed us to better investigate the therapeutic effects of Abn-CBD in T1D as well as to strengthen the findings on the pathways and processes involved.

2. Materials and methods

2.1. Materials

Abn-CBD was purchased from Tocris (Biogen). Streptozotocin (STZ), 5-Bromo-2'-deoxyuridine (BrdU), and Fluoroshield mounting media with DAPI were purchased from Sigma Aldrich. Antigen Unmasking Solution (H-3300) and DAB Peroxidase Substrate were purchased from Vector Laboratories. Trichrome Stain Kit was purchased from Abcam. Primary antibodies used were mouse anti-BrdU (1:50; G1G2) from the Hybridoma Bank, mouse anti-insulin (1:500; I2018) from Sigma Aldrich, rabbit anti-insulin (1:100; sc-9168) from Santa Cruz Biotechnology, rabbit anti-cleaved caspase 3 (1:100; #9661) from Cell Signaling, rat anti-F4/80 (1:100; ab6640) and rabbit anti-TXNIP (1:100; ab188865), anti-NF-kB p65 (phospho S536; 1:100; ab86299), anti-CD3 (1:100; ab5690), anti-CD163 (1:500; ab182422) and anti-iNOS (1:100; Ab15323) from Abcam, and ready-to-use mouse anti-CD4 and rabbit anti-CD8 (both undiluted) from Ventana. Secondary antibodies were anti-mouse Alexa Fluor 488, anti-mouse Alexa Fluor 568, anti-rabbit Alexa Fluor 488 and rabbit Alexa Fluor 568 (1:1000; Thermo Fisher Scientific).

2.2. Animals

Animal care and procedures were approved by the Animal Experimentation Ethics Committee of the Malaga University and authorized by the government of Andalucia (Project number 28/06/2018/107). The European directive 2010/63/EU on the use of animals for research purposes was followed, as well as the ARRIVE 2.0 guidelines on reporting experiments involving animals or animal tissue. Mice were housed in groups of 10 using 12 h dark/light cycles and provided regular chow (SAFE A04, Panlab) and water ad libitum. Eight-to-ten-week-old C57BL6J male and 6-week-old NOD/ShiLtJ female mice were purchased from Charles River France and Italy, respectively. NOD/ShiLtJ female littermate mice were randomly assigned to 3 groups: vehicle, 0.1 or 1 mg/kg of Abn-CBD. Mice were daily i.p. injected with vehicle or various dosages of Abn-CBD for 3 months. At the end of the study, mice were euthanized by cervical dislocation, and tissues and blood were collected and processed immediately for histological and biochemical analysis. C57BL6J male littermate mice were randomly assigned to 2 groups: vehicle or Abn-CBD. Mice were injected daily with i.p. injections of vehicle (saline:DMSO:Tween-80 95:4:1) or 1 mg/kg of Abn-CBD for 7 days. Mice were then fasted for 4 h, injected i.p. with 150 mg/kg of streptozotocin (STZ), and given 10% sucrose water for 48 h to avoid hypoglycemia. Blood glucose was monitored daily using OneTouch Ultra blood glucose meter (LifeScan IP Holdings, LLC). After 6 days, mice were hyperglycemic (mean blood glucose level was 382 ± 19.4 mg/dl). Mice were injected with BrdU and euthanized by cervical dislocation the following day.

2.3. Intraperitoneal glucose tolerance test

A glucose tolerance test was performed as previously described [23]. Briefly, after 6 weeks of treatment (mid-study) NOD mice were fasted overnight (16 h) and given water ad libitum prior to an i.p. injection with a bolus of 2 g/kg of glucose. Blood glucose from tail bleeds was analyzed at 0, 15, 30, 60, and 90 min after being given the bolus.

2.4. Histopathology of pancreas

Pancreata were dissected and fixed in methanol-free 4% paraformaldehyde for 24 h at 4 °C, and then paraffin-embedded. For

immunohistochemistry, 5 μm sections were dewaxed, rehydrated, and subjected to heat-mediated citric acid-based antigen retrieval for 20 min in a preheated steamer, followed by additional 20 min of cooling down. For DAB staining, peroxidase activity was blocked for 10 min with 3% hydrogen peroxide. Sections were blocked in 5% goat or donkey serum or bovine serum albumin (BSA) 0.3% Triton-X-100 in PBS for 30 min at 37 °C. Slides were then incubated with primary antibody diluted in 1% serum or BSA, 0.3% Triton-X-100 in PBS overnight at 4 °C, washed 3 times for 5 min in 0.3% Triton-X-100 PBS, incubated with secondary antibody diluted in 1% serum or BSA, 0.3% Triton-X-100 in PBS for 30 min at 37 °C and then washed 3 times for 5 min in 0.3% Triton-X-100 PBS. Alexa Fluor or HRP polymer-conjugated antibodies were incubated for 45 min at 37 °C, and nuclei stained using DAPI for immunofluorescence. DAB staining was performed following hematoxylin for nuclei staining. Negative controls were performed using 0.3% Triton-X-100 PBS containing 1% goat serum or BSA. For Masson's trichrome staining, 5 μm sections were dewaxed, rehydrated, and stained using Trichrome Staining Kit following the manufacturer's instructions. Imaging was performed at 200X using an Olympus BX41. BrdU and insulin co-staining images were obtained using a Leica SP5 II confocal microscope.

2.5. Image analysis

Densitometric analysis of images was performed using ImageJ (NIH). The percentage of proliferating beta-cells per islet was determined counting the number of BrdU-insulin-positive cells. Images from DAB staining were submitted to color deconvolution using the Hematolxylin/DAB vector from ImageJ Fiji, and the resulting DAB channel (R:0.26, G:0.57, B:0.77) was quantified. Similarly, images from trichrome staining were color deconvoluted and the area of islets with blue (collagen; deconvoluted channel R: 0.83, G: 0.51, B: 0.19) signal was quantified by Image J software. Infiltration of immune cells in the STZ-hyperglycemic model was quantified by counting the number of positively stained cells per islet. N = 10–15 islets per mouse from a total of N = 7–9 mice per group from 3 non-consecutive pancreatic sections, i.e. N = 90–100 islets per group).

2.6. Insulitis determination

Pancreata from NOD mice were analyzed by histochemistry after insulin and hematoxylin staining for insulitis as per the following grades: grade 0 (no infiltration; healthy islets), grade 1 (immune cells approach the islet but do not infiltrate it; activation of the inflammatory response has started), grade 2 (immune cells infiltrate around the islet), and grade 3 (immune cells infiltrate into the islet; beta cell destruction occurs) (Fig. 1B).

2.7. $CD4^+$ T cell isolation

Blood samples from the final bleed of NOD mice were collected in tubes containing heparin. $CD4^+$ T cells were isolated using EasySep Mouse CD4 + T Cell Isolation Kit (Stemcell technologies) following the manufacturer's instructions. Briefly, red blood cells lysis was achieved with 0.8% ammonium chloride. Cells were washed with Ca^{+2}- Mg^{+2}-free PBS containing 2% fetal bovine serum (FBS) and 1 mM EDTA and resuspended at 1×10^8 cells/ml. Samples were incubated with rat serum and isolation cocktail (1:40) for 10 min at room temperature. Then, samples were incubated with streptavidin-coated magnetic particles (RapidSpheres) for 2.5 min at room temperature and negative isolation was performed using an EasySep magnet (#18000, Stemcell technologies). Isolated $CD4^+$ T cells were pelleted and flash frozen.

2.8. RNA purification and real-time PCR

Freshly isolated $CD4^+$ T cells from NOD mice were homogenated in TRI Reagent (Sigma Aldrich) and total RNAs extracted. Total RNA concentration and quality were measured by Nanodrop (Thermo Fisher Scientific). Reverse transcription was performed using SuperScript IV Reverse Transcriptase in 20 μl (Thermo Fisher Scientific). Relative expression of *Cd4* (Mm00442754_m1), *Tnfa* (Mm00443258_m1), *Ifng* (Mm01168134_m1), *Il4* (Mm00445259_m1), Il10 (Mm01288386_m1), *Il17a* (Mm00439618_m1), and *Il21* (Mm00517640_m1) genes was assayed using TaqMan Fast Advanced Master Mix and FAM-labeled hydrolysis probes from TaqMan Gene Expression Assays, all probes span exon junctions, in a total volume of 20 μl (Thermo Fisher Scientific) for each specific gene on an ABI 7500 real-time PCR System (Thermo Fisher Scientific). PCR protocol was 2' at 50 °C (hold), 2' at 95 °C (hold) and 40x cycles of 3'' at 95 °C and 30'' at 60 °C. Fast Duplex reactions were performed using VIC-labeled β-actin (reference gene) for endogenous control.

2.9. Cytokines measurements

Blood samples from STZ-challenged and NOD mice were collected in tubes containing EDTA and plasma separated by centrifugation. Plasma samples were flash-frozen and kept at −80 °C. Cytokines (Il-6, TNFα, CXCL-1, CXCL-2, MCP-1) were determined using a ProcartaPlex Immunoassay (Thermo Fisher Scientific). When plasma samples were not sufficient for analysis, two samples from the same group were pooled together (stated in the figure legend).

2.10. Flow cytometry

Pancreatic lymph nodes (PLN) from STZ-challenged mice were dissected as previously described [24] and mechanically disaggregated in media (RPMI). Erythrocytes were lysed incubating cells with ACK lysis buffer for 3 min at room temperature. Cells were immediately washed 3 times with media and plated at a density of 4×10^6 cells/ml in a 96-well plate. Cells were stained using PerCP anti-mouse CD3 (1:25) and APC anti-mouse CD4 (1:100; Biolegend) during 20 min at room temperature. Cells were washed with FACS Flow, fixed in 4% paraformaldehyde, and washed with Perm/Wash Buffer (BD Biosciences) before staining with APCCy7 anti-mouse IFNγ (1:10; Biolegend). Appropriate isotype controls were used in all the experiments. Populations were determined by using BD FACS Canto II and the FACS Diva software (BD Biosciences).

2.11. Statistical analysis

Data are shown as mean ± SEM, including individual values. Statistical analysis was performed using GraphPad Prism version 6.07. The normal distribution of data was assessed by normality tests. Mean values were compared using Student's *t*-test or Mann-Whitney test for two groups comparisons, and ANOVA with Tukey's or Dunn's test for multiple comparisons, for the parametric or non-parametric test, respectively. Survival curves were compared using the two-group Mantel-Cox test. A p-value < 0.05 was considered significant.

2.12. Randomization

Littermates were randomly assigned to vehicle or treatment groups.

2.13. Blinding

Samples were coded and analysis of plasma and images were blinded to the analyst.

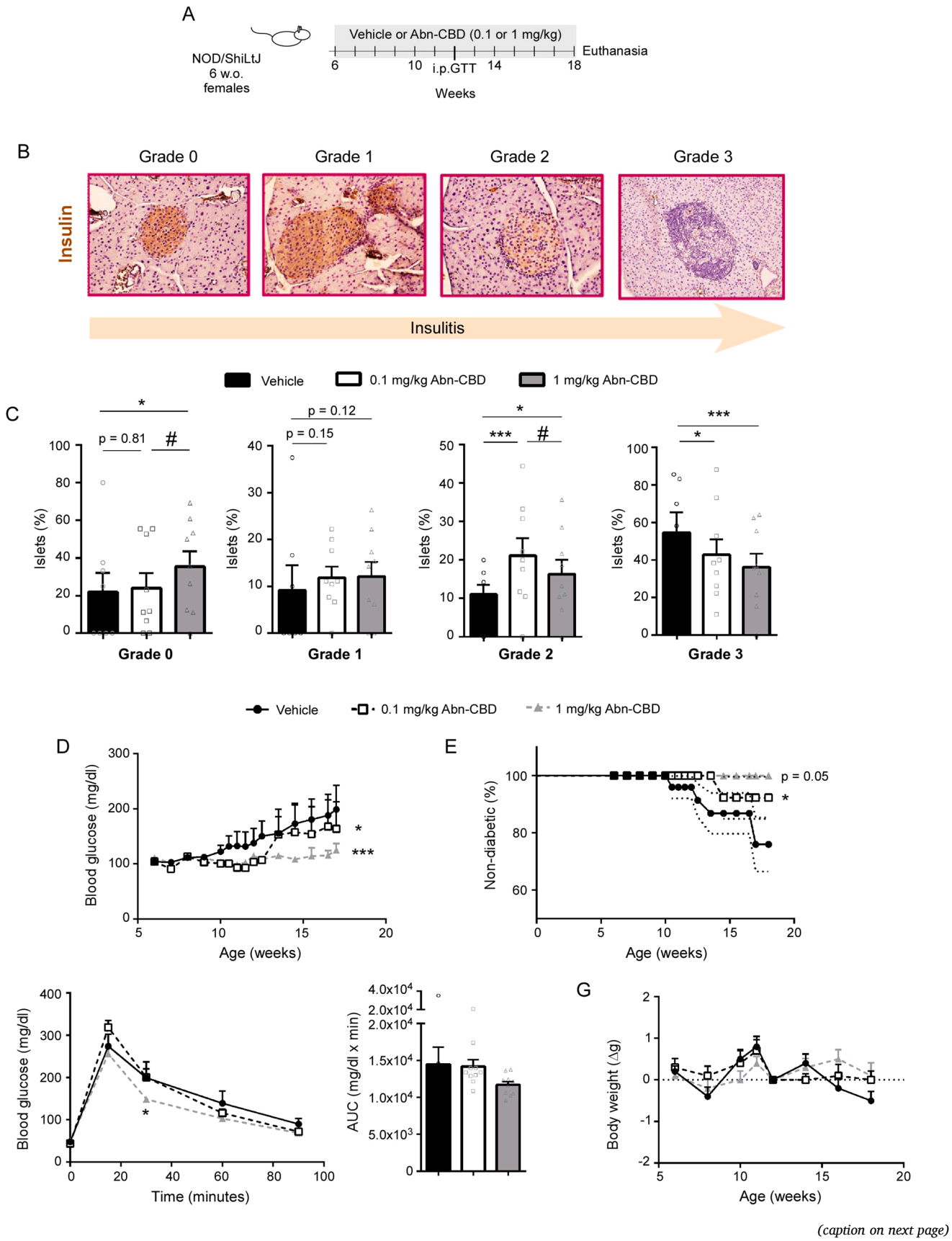

(caption on next page)

Fig. 1. Insulitis grade and diabetic phenotype in NOD mice treated with Abn-CBD. (A) Schema of the experimental procedure. Six-week-old non-obese diabetic (NOD) mice were treated with Abn-CBD or vehicle for 3 months, and mice were sacrificed at 18-week-old and pancreas dissected, formalin-fixed, and paraffin-embedded. (B) Pancreas sections were immunostained for insulin and counterstained with hematoxylin. Distinct grades of insulitis were: grade 0 = no immune cell infiltration, insulin is preserved; grade 1 = immune cells approaching the islet, insulin is preserved; grade 2 = immune cells around the islet, islet start to lose insulin content; grade 3 = immune cells inside the islet, insulin is almost, or totally, lost. (C) Quantification of insulitis by determining the percentage of islets in each grade. Data are mean ± S.E.M of vehicle- (black bars), 0.1 mg/kg Abn-CBD (white bars) and 1 mg/kg Abn-CBD-treated (grey bars) mice. Individual data are shown (dots). N = 7–9 mice per group, N = 100 islets per group. * $p < 0.05$ and * **$p < 0.001$ compared to vehicle, # $p < 0.05$ compared to 0.1 mg/kg of Abn-CBD. (D) Blood glucose and (E) incidence of T1D in NOD mice treated with Abn-CBD or vehicle. The onset of diabetes was considered when blood glucose > 250 mg/dl for 2 consecutive days. The dotted lines show interindividual variability within each group. (F) Blood glucose during an intraperitoneal glucose tolerance test (i.p.GTT) in NOD mice treated with Abn-CBD or vehicle for 6 weeks (mid-study), and area under the curve (AUC; individual data are shown -dots-). (G) Bodyweight changes in NOD mice treated with Abn-CBD or vehicle. Data are mean ± S.E.M of vehicle- (black bars, black circles with solid line), 0.1 mg/kg Abn-CBD (white bars, white squares with dotted line) and 1 mg/kg Abn-CBD-treated (grey bars, grey triangles with dotted line) mice. N = 10 mice per group. * $p < 0.05$ compared to vehicle. Non-significant p values are shown compared to vehicle.

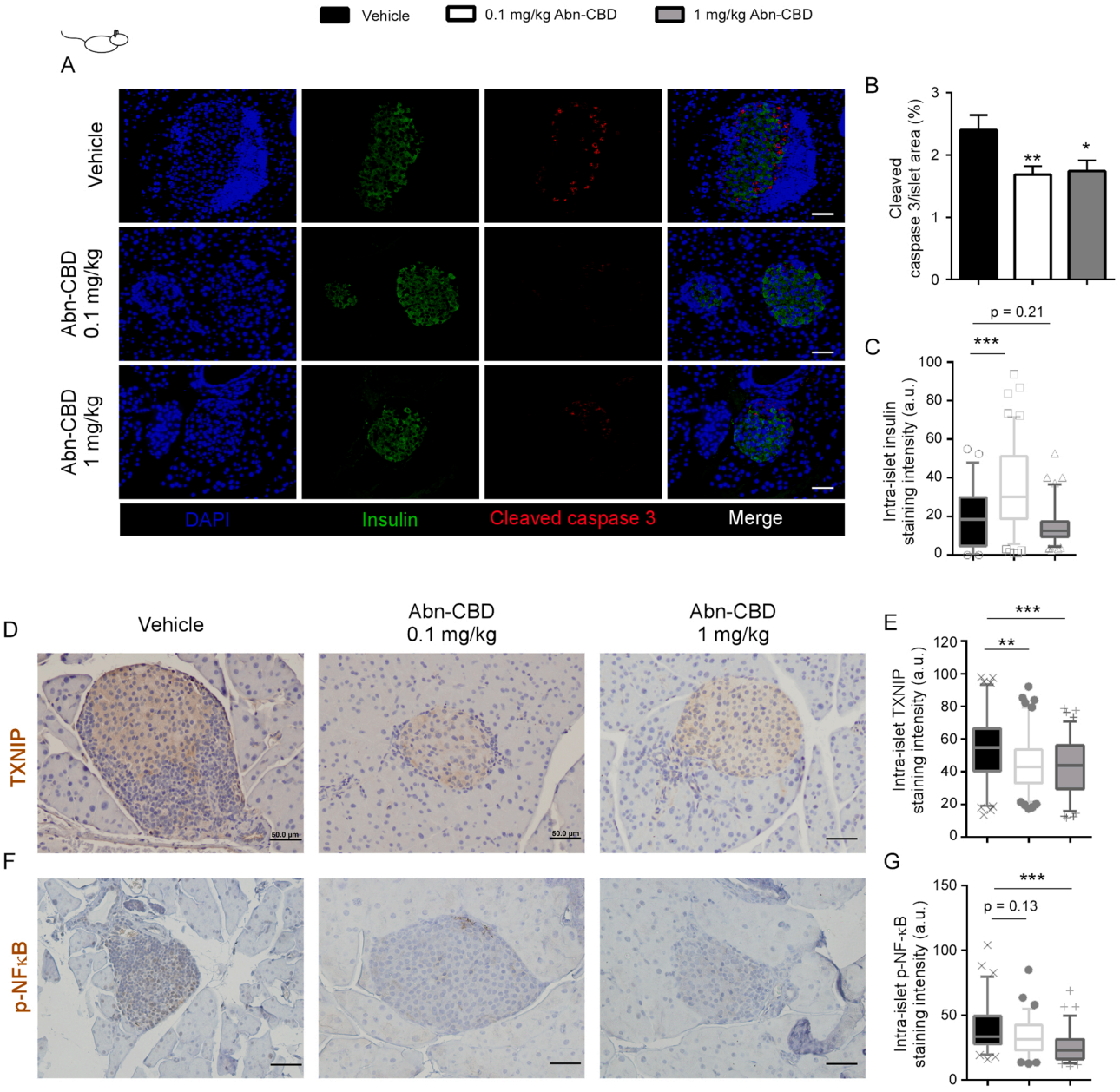

Fig. 2. Apoptosis and inflammation of islet cells in NOD mice treated with Abn-CBD. (A) Representative images of the pancreas of NOD mice treated with vehicle, 0.1 or 1 mg/kg of Abn-CBD immunostained for cleaved caspase 3 (red), insulin (green) and DAPI (blue) and (B) quantification of islet cell apoptosis and (C) intra-islet insulin staining. Representative images and quantification of pancreas sections immunostained for (D-E) TXNIP and (F-G) p-NF-κB. Data are mean ± S.E.M (bars) or box & whiskers plot with 10–90 percentile of vehicle- (black bars), 0.1 mg/kg Abn-CBD (white bars), and 1 mg/kg Abn-CBD-treated (grey bars) mice. The scale bar is 50 μm. N = 7–9 mice per group, N = 90–100 islets per group. * $p < 0.05$, * *$p < 0.01$ and * **$p < 0.001$ compared to vehicle. Non-significant p values are shown compared to vehicle.

3. Results

3.1. Abn-CBD reduces the severity of insulitis in NOD mice

The non-obese diabetic (NOD) mouse is considered the gold standard model of T1D. In NOD mice, there is a spontaneous autoimmune attack -insulitis- predominantly in females that initiates at around 5 weeks of age, and eventually spreads all over the pancreas by 12 weeks of age, presenting overt T1D; its median incidence is 18 weeks of age [25]. The impact of Abn-CBD was assessed in this robust model to investigate its capacity to ameliorate immune cells' over-reactivity, i.e. insulitis, using dosages previously described by others and by us to efficiently regulate blood glucose and inflammation in rodents [17,26,27]. Six-week-old mice were treated i.p. with 0.1 or 1 mg/kg of Abn-CBD or vehicle for 12 weeks and blood glucose was monitored weekly (Fig. 1A). An i.p. glucose tolerance test was performed after 6 weeks of treatment. At the end of the study, mice were sacrificed and pancreata analyzed by histochemistry for insulitis. The lower dose (0.1 mg/kg) of Abn-CBD reduced the progression of insulitis, increasing the number of islets in grade 2 of insulitis (21 ± 4 vs. 11 ± 2%) while reducing grade 3 (42 ± 8 vs. 54 ± 10%) compared to vehicle-treated mice (Fig. 1C). A higher dose of Abn-CBD (1 mg/kg) further reduced the number of islets in grade 3 of insulitis (36 ± 7 vs. 54 ± 10%), and, importantly, showed a significant increase of healthy (grade 0) islets (35 ± 8 vs. 25 ± 11%) (Fig. 1C). NOD mice treated with both dosages of Abn-CBD had lower blood glucose over the course of the study (Fig. 1D) and also showed a dose-dependent delay on the onset of T1D (onset of diabetes was considered when non-fasting blood glucose > 250 mg/dl for 2 consecutive days [28]) (Fig. 1E). An intraperitoneal (i.p.) glucose tolerance test showed that treatment with 1 mg/kg of Abn-CBD also improved glucose tolerance, as shown by a significantly lower blood glucose level 30 min after giving the bolus of glucose (Fig. 1F). No significant changes were found in body weight (Fig. 1G).

3.2. Abn-CBD reduces activation of islet TXNIP-NF-κB pathway in NOD mice, ameliorating islet cells apoptosis

Insulitis leads to loss of beta cells and consequent loss of insulin; thus, we investigated if the changes in immune cells infiltration were reflected in the preservation of beta cell mass. Treatment with 0.1 mg/kg of Abn-CBD reduced 1.5-fold islet cell apoptosis compared to vehicle and assessed by co-immunostaining of the pancreas with insulin and cleaved caspase 3 (Fig. 2A–B). One mg/kg of Abn-CBD reduced islet cell apoptosis to the same extent as 0.1 mg/kg dose (Fig. 2A–B). Quantification of insulin staining showed that, although mice from all groups had islets with no insulin staining, treatment with 0.1 mg/kg of Abn-CBD significantly increased insulin content compared to others (Fig. 2C). Thioredoxin-interacting protein (TXNIP), which is an activator of the inflammasome, triggers beta cell death in T1D and T2D [29–32]. In parallel, activation of the inflammasome by TXNIP also induces the phosphorylation of the p65 subunit of NF-κB, resulting in its nuclear translocation and increased expression of proinflammatory cytokines, which are then processed and activated by the inflammasome [33,34]. Thus, we assessed whether Abn-CBD targeted TXNIP and NF-κB signaling pathways. Both dosages of Abn-CBD significantly reduced, to the same extent, TXNIP levels in islets of NOD mice (Fig. 2D–E), and 1 mg/kg of Abn-CBD also induced a significant 1.5-fold reduction in the phosphorylation of NF-κB (Fig. 2F–G). Taken together, treatment of NOD mice with Abn-CBD significantly reduced islet inflammation, decreasing the peri- and intra-islet infiltration of immune cells, thus improving islet survival.

3.3. Abn-CBD ameliorates the systemic inflammatory profile in T cells from NOD mice

There is a systemic chronic inflammation in T1D associated with high levels of circulating TNFα among other pro-inflammatory cytokines, and Il-6 in the late stage of the disease [35]. We analyzed the levels of circulating cytokines and chemokines in the NOD mice treated with Abn-CBD compared to vehicle-treated NOD mice. We did not detect Il-6 in the plasma of any group. Despite a tendency to decreased TNFα and CXCL-2 levels in the 0.1 mg/kg Abn-CND-treated NOD mice (Fig. 3A,B), there were no significant changes in the levels of TNFα, CXCL-2, MCP-1, and CXCL-1 in the Abn-CBD-treated compared to vehicle-treated NOD mice (Fig. 3A–D). In the early stage of T1D, naïve $CD4^+$ cells are polarized to Th1 T cells, increasing the Th1/Th2 ratio. Th1 $CD4^+$ T cells secrete the pro-inflammatory cytokines IFNγ and TNFα, which induce the differentiation of $CD8^+$ T cells to CTL. CTLs infiltrate the islets of Langerhans and induce beta cell death by secreting granzymes and perforins. Since we found a significant reduction in the insulitis upon treatment with Abn-CBD despite not revealing any significant changes on circulating cyto/chemokines, we further analyzed the inflammatory profile of Th cells. $CD4^+$ T cells were isolated and the expression of cytokines mRNA was analyzed. The purity of $CD4^+$ T cells was determined by the expression of *Cd4* (Fig. 3E). Treatment with Abn-CBD lowered the expression of *Il10* (Treg cell marker; Fig. 3F), *Ifng* (Th1 cell marker; Fig. 3G), and *Il21* (Th17 cells marker; Fig. 3H), independently of the dose. $CD4^+$ T cells from mice treated with 1 mg/kg Abn-CBD further showed significantly lower expression of *Tnfa* (Fig. 3I). Expression of *Il4* was virtually absent in circulating $CD4^+$ T cells from vehicle- or 0.1 mg/kg Abn-CBD-treated mice, while it was expressed in $CD4^+$ T cells from 1 mg/kg Abn-CBD-treated mice (Fig. 3J). Altogether, the data indicate a reduction in the pro-inflammatory profile of $CD4^+$ T cells in Abn-CBD-treated compared to vehicle-treated NOD mice.

3.4. Abn-CBD reduces streptozotocin-induced islet cells apoptosis without altering islet structure

In T1D beta cells undergo countless stress stimuli, inflammation, and apoptosis. STZ is a widely used drug to induce beta cell damage, since it preferably gets internalized through GLUT2, induces reactive oxygen species (ROS), and provokes an inflammatory response that ultimately leads to beta cell death, islet damage, and hyperglycemia [36]. STZ also increases islet size and apoptosis (Fig. S1, [37]). We used this model to assess the impact of the higher and most effective dose of Abn-CBD, 1 mg/kg, to protect from an acutely-induced beta cell damage. C57BL6J mice were pretreated with 1 mg/kg of Abn-CBD or vehicle (saline:DMSO:Tween-80) during 7 days, before the STZ challenge. Mice were injected with BrdU 6 days after STZ injections and were then euthanized 24 h after (Fig. 4A). Abn-CBD pre-treated mice had a significantly higher number of small islets correlating with a slightly lower average islet size compared to vehicle-treated mice (Fig. 4B–C). We did not find significant changes in intra-islet insulin staining (Fig. 4D) nor in beta cell proliferation (Fig. 4E–F). However, a significant 1.9-fold reduction in islet cell apoptosis was detected in Abn-CBD pre-treated mice compared to vehicle, as shown by a reduction in intra-islet cleaved caspase 3 staining (Fig. 4G–H). Thus, pretreatment with Abn-CBD protects small-size islets from damage and decreases beta cell death.

3.5. Abn-CBD attenuates TXNIP and NF-κB pathways and circulating pro-inflammatory cytokines

STZ was previously shown to induce the expression of TXNIP; [29] moreover, activation of TXNIP and NF-κB pathways synergize promoting beta cell death and fibrosis [34,38]. Intra-islet TXNIP staining was significantly reduced (Fig. 5A-B) with a concomitant 1.6-fold reduction in the activation of NF-κB in Abn-CBD-treated versus untreated mice (Fig. 5C–D). Accordingly, fibrosis was reduced by 1.6-fold in islets from mice pre-treated with Abn-CBD compared to vehicle-treated mice (Fig. 5E–F). In parallel, circulating plasma levels of the proinflammatory cytokines IL-6 and TNFα, as well as the chemokine CXCL-2, were

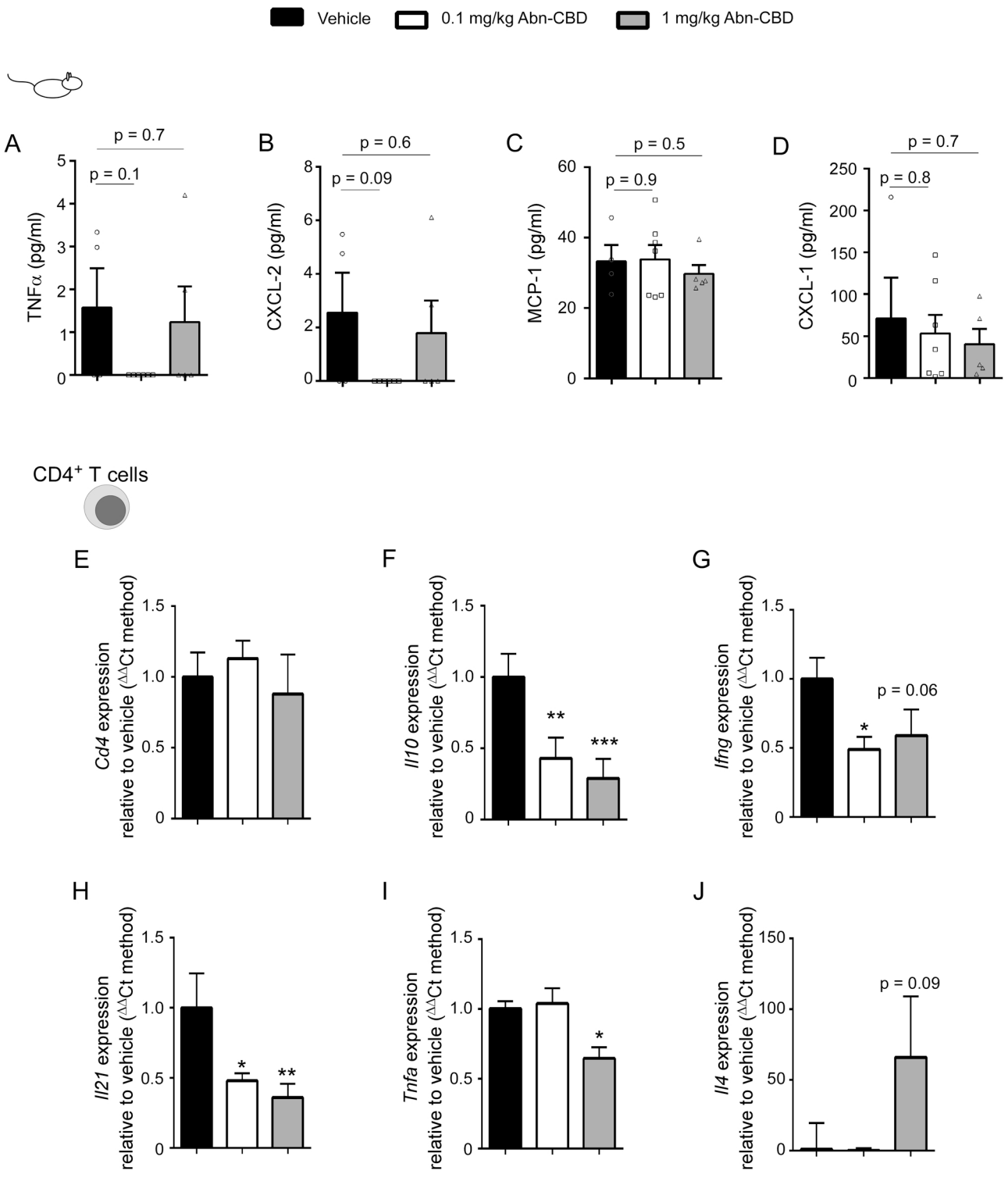

Fig. 3. Circulating cytokines and expression profile of circulating $CD4^+$ T cells in NOD mice treated with Abn-CBD. Plasma levels of (A) tumor necrosis factor alpha (TNF-α), (B) chemokine ligand 2 (CXCL-2), (C) monocyte chemoattractant protein-1 (MCP-1) and (D) CXCL-1 in NOD mice treated with vehicle, 0.1 or 1 mg/kg of Abn-CBD. Data are mean ± S.E.M of vehicle- (black bars), 0.1 (white bars), and 1 mg/kg (grey bars) Abn-CBD-treated mice. N = 5–7 mice per group. Non-significant p values are shown compared to vehicle. $CD4^+$ T cells were isolated from NOD mice treated with vehicle, 0.1 or 1 mg/kg of Abn-CBD. (E) The expression of *Cd4* was used as control. Expression of (F) interleukin 10 (*Il10*), (G) interferon gamma (*Ifng*), (H) interleukin 21 (*Il21*), (I) *Tnfa* and (J) interleukin 4 (*Il4*) in $CD4^+$ T cells. Data are mean ± S.E.M of vehicle- (black bars), 0.1 (white bars) and 1 mg/kg (grey bars) Abn-CBD-treated mice. N = 10 mice per group. * $p < 0.05$, * *$p < 0.01$ and * **$p < 0.001$ compared to vehicle. Non-significant p values are shown compared to vehicle.

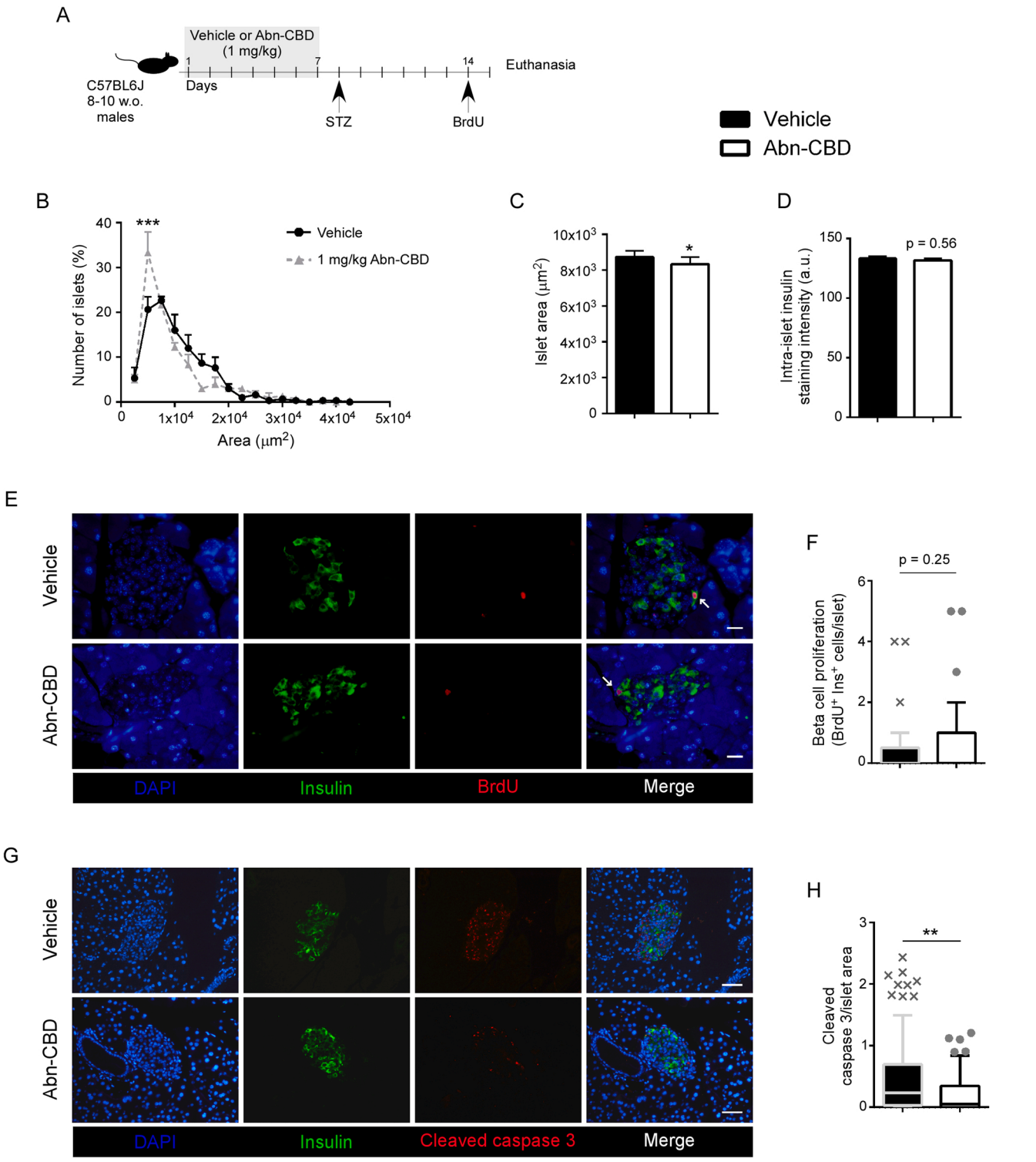

Fig. 4. Effect of Abn-CBD on islet structure in STZ-induced hyperglycemic mice. (A) Schema of the experimental procedure. Seven days Abn-CBD- and vehicle-treated mice were injected with streptozotocin (STZ), sacrificed one week later and pancreas dissected, formalin-fixed paraffin-embedded. Analysis of (B) islet area frequency distribution and (C) mean islet area per group. Pancreas sections were immunostained for insulin and (D) quantified. (E) Representative images of pancreas immunostained for BrdU (red), insulin (green) and DAPI (nuclei, blue) and (F) quantification of beta cell proliferation. (G) Representative images of pancreas immunostained for cleaved caspase 3 (red), insulin (green) and DAPI (blue), and (H) quantification of islet cell apoptosis. Data are mean ± S.E.M (bars) or box & whiskers plot with 10–90 percentile of vehicle- (black bars, black circles, and solid line) and Abn-CBD-treated (white bars, grey triangles with dotted line) mice. The scale bar is 20 (E) and 50 μm (G). N = 9 mice per group, N = 90–100 islets per group. * $p < 0.05$, * *$p < 0.01$, and * **$p < 0.001$ compared to vehicle. Non-significant p values are shown compared to vehicle. (For interpretation of the references to colour in this figure, the reader is referred to the web version of this article.)

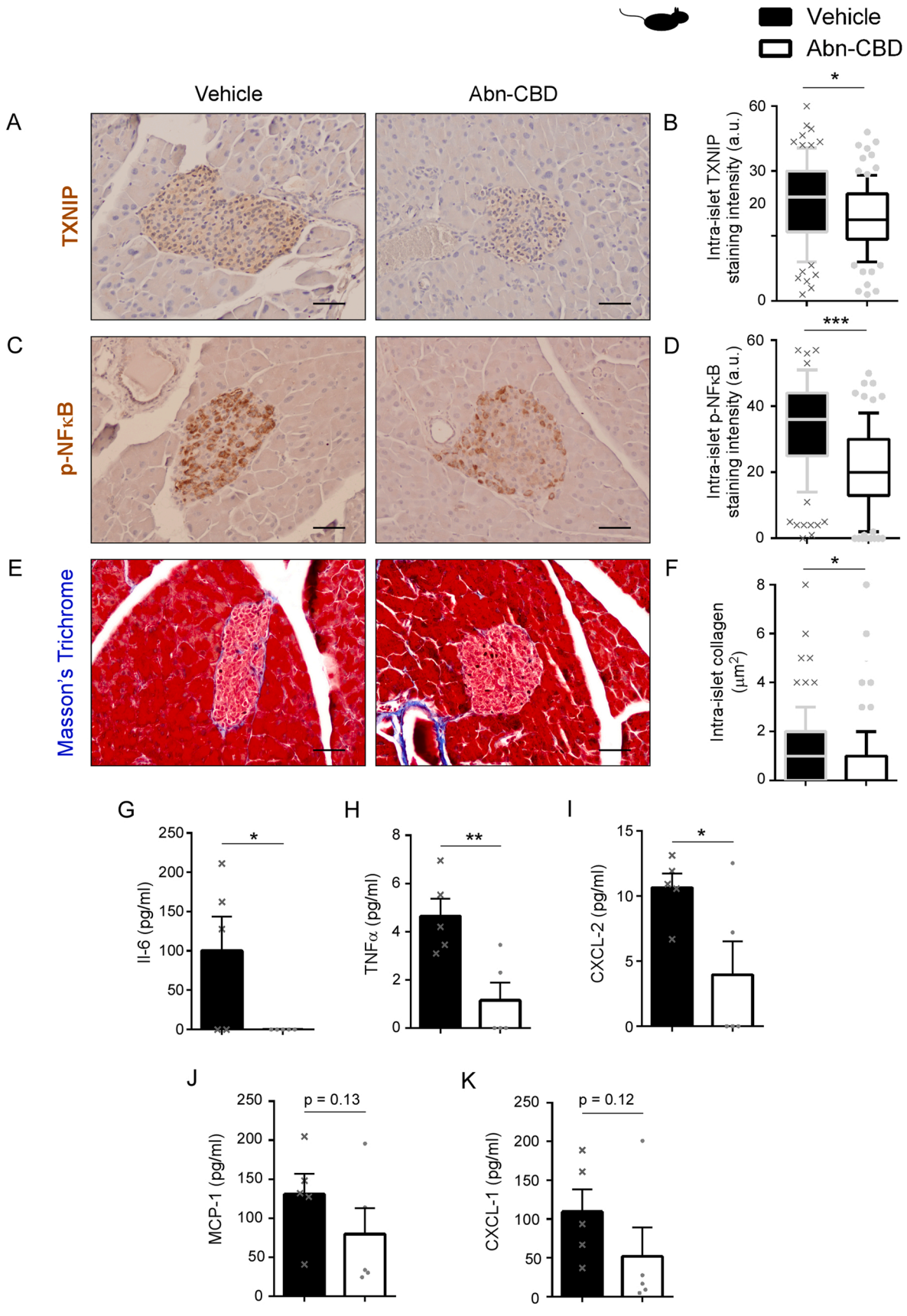

(caption on next page)

Fig. 5. Effects of Abn-CBD on intra-islet and systemic inflammation in STZ-induced hyperglycemic mice. Representative images and quantification of pancreas sections immunostained for (A-B) TXNIP and (C-D) phospho-NF-κB. (E) Representative images of pancreas sections stained to visualized the connective tissue (blue), nuclei (purple), and cytoplasm (pink) by Masson's Trichrome staining. (F) Quantification by Image J FIJI of intra-islet collagen (blue staining) content upon image color deconvolution. Data are shown in box & whiskers plot with 10–90 percentile of vehicle- (black bars) and Abn-CBD-treated (white bars) mice. The scale bar is 20 μm. N = 9 mice per group, N = 90–100 islets per group. * $p < 0.05$, * *$p < 0.01$, and * **$p < 0.001$ compared to vehicle. Blood samples from the final bleed were collected and plasmatic levels of cytokines were measured. (G) Plasma levels of Interleukin 6 (IL-6), (H) tumor necrosis factor alpha (TNF-α), (I) chemokine ligand 2 (CXCL-2), (J) monocyte chemoattractant protein-1 (MCP-1), and (K) CXCL-1 in STZ-induced hyperglycemic mice pretreated with Abn-CBD or vehicle. Data are mean ± S.E.M of vehicle- (black bars) and Abn-CBD-treated (white bars) mice. Individual data are shown (dots). N = 5 samples corresponding to pools of 2 mice each, N = 9 mice per group. * $p < 0.05$ and * *$p < 0.01$ compared to vehicle. Non-significant p values are shown compared to vehicle.

significantly reduced in Abn-CBD-treated mice compared to vehicle-treated mice (Fig. 5G–I). In comparison to NOD mice, STZ-treated mice showed increased levels of Il-6, a 2.8-fold increase of TNFα, 4.2-fold increase of CXCL-2, 3.9-fold increase of MCP-1, and a 1.5-fold increase of CXCL-1 (Figs. 3A–D, 5E–F), most probably due to the acuteness of the insult. Interestingly, levels of IL-6 were undetectable in the plasma of Abn-CBD treated mice. No significant changes were detected in the levels of MCP-1 and CXCL-1 in mice treated with Abn-CBD compared to vehicle (Fig. 5J-K). Taken together, these results indicate that Abn-CBD decreases circulating pro-inflammatory cytokines as well as enhances islet survival, ameliorating the TXNIP and NF-κB pathways.

3.6. Abn-CBD alleviates the pro-inflammatory profile of islet immune cells in STZ-treated mice

Although resident immune cells exist in islets of Langerhans, islets from non-diabetics show virtually no $CD8^+$ T nor $CD4^+$T cells compared to diabetics [39,40], and STZ recruits T cells into islets of Langerhans (Fig. S1, [41]). Since Abn-CBD dampens the expression of TXNIP and NF-κB activation, as well as circulating levels of proinflammatory chemo- and cytokines -indicative of inflammatory resolution-, we next assessed the profile of the immune cells within the islets. Although no significant changes in the overall islet macrophage ($F4/80^+$) population was detected ($p = 0.17$; Fig. 6A-B), the anti-inflammatory M2 sub-populations ($CD163^+$) was slightly lower in Abn-CBD-treated compared to vehicle-treated mice (Fig. 6C–D), and there was a significant 2.4-fold reduction in the number of proinflammatory M1 macrophages ($iNOS^+$; Fig. 6E–F). The number of T cells ($CD3^+$) infiltrated into the islets was 1.8-fold lower in islets of mice pretreated with Abn-CBD (Fig. 6G–H). Further analysis for T cell types showed a 2-fold reduction in the intra-islet number of $CD8^+$ T cells in mice pre-treated with Abn-CBD compared to vehicle-treated mice (Fig. 6I–J). The overall T helper (Th; $CD4^+$)-cell population remained constant between groups (Fig. 6K–L). $CD4^+IFNg^+$ (Th1)/$CD4^+IFNg^-$ (non-Th1) ratio was assessed in pancreatic lymph nodes (PLN) from these mice. Abn-CBD abolished the STZ-induced increase of the Th1/non-Th1 ratio (Fig. 6M). Thus, Abn-CBD appears to blunt Th1-mediated response, correlating with lower islet cell apoptosis.

4. Discussion

Phytocannabinoids and synthetic cannabinoids have been investigated due to their anti-inflammatory and glucose-lowering properties, but their potential as therapeutic agents for the treatment of insulitis and T1D remains largely unexplored. Herein we investigated the potential pre-clinical benefits of the synthetic cannabinoid Abn-CBD in a T1D mouse model (NOD mice) and a beta cell-damaged model (STZ-insulted mice), as emerging evidence points to its ability in modulating inflammation, insulin secretion as well as beta cell proliferation and apoptosis [17,18,26,27]. Overall, we found that prophylactic administration of Abn-CBD was able to 1) reduce levels of circulating pro-inflammatory cytokines, 2) reduce $CD4^+$ T cells pro-inflammatory profile, 3) decrease intra-islet inflammation and immune cell infiltration in the islets, reducing the severity of insulitis and 4) decrease apoptosis, hence protecting and preserving islets of Langerhans. These actions of Abn-CBD are compatible with an improved intra-islet environment, potentially preserving islet function.

Treatment with Abn-CBD delayed the progression of insulitis in NOD mice, decreased blood glucose levels, and improved glucose tolerance, slightly delaying the onset of T1D. Long-term treatments of NOD mice are warranted to elucidate to which extent Abn-CBD is capable of delaying the progression of the disease. Our data suggest an improved intra-islet environment. Indeed, using STZ to acutely damage beta cells, we found that Abn-CBD significantly increased the percentage of small islets compared to vehicle-treated mice, also suggesting that Abn-CBD may be specifically protecting these small islets that are known to be more sensitive to damage during T1D [42]. A similar effect on islet size had been previously found in Abn-CBD-treated diet-induced pre-diabetic mice [26].

Other synthetic cannabinoids have been shown to protect beta cells from various insults: cytokines, high-fat diet, hyperglycemia, STZ, etc [10,18,26]. During T1D progression, beta cell damage is a key feature that eventually leads to loss of functional beta cell mass, hence, overt diabetes, and its preservation is key. We have recently described that (+)-CBD-HPE, a (+) enantiomer of CBD, protects against STZ-mediated beta cell apoptosis and inflammation [37]. Here we report that Abn-CBD significantly reduced islet cells apoptosis in both models studied (spontaneous NOD diabetic mice and beta cell-damaged by STZ-challenge), in agreement with previous reports in mouse models of T2D [18,19,26], in which Abn-CBD was shown to reduce cytokine (mix of TNFα, IFNγ and IL-1β)-induced apoptosis in islets in vitro [18]. IL-6, which is elevated in T1D [3], plays a very important role at the onset of T1D by activating $CD4^+$ T cell differentiation [43]. Abn-CBD greatly reduced circulating levels of proinflammatory cytokines in our model and others [26], including IL-6, whose levels were, in fact, undetectable. Accordingly, $CD4^+$ T cells from Abn-CBD-treated NOD mice expressed significantly less *Tnfa* and *Ifng* than vehicle-treated NOD mice. Moreover, expression levels of *Il21*, a cytokine secreted by Th17, were also decreased in NOD mice. Th17 cells have been considered as a central player in T1D development, which enhances the autoimmune response that leads to insulitis by further stimulating $CD8^+$ cells differentiation into CTL cells [44]. Thus, decreased *Il21* expression further supports the establishment of an anti-inflammatory environment. This mechanism was also observed, to a lower extent due to the acuteness condition of the model and early stages, in the STZ model, in which Abn-CBD-treated mice also harbored a decreased number of T cells in the islets as well as a lower Th1/non-Th1 $CD4^+$ cell ratio, both involved in CTL cells expansion. We also observed decreased expression of *Il10*, which is secreted by Tregs, in addition to Th2 cells. Changes in *Il10* may be attributed to a modulation of Tregs, but little is known about the role of Tregs in T1D. Defects in Treg function are associated with T1D [45], although no changes in Treg population have been found in patients with T1D [46]. Further studies regarding the potency of Abn-CBD to regulate these different T cell populations are necessary.

Macrophages can further amplify the inflammatory response by recruiting other immune cells such as lymphocytes. Because resident macrophages exist within the islets, an acute insult to damage beta cells such as STZ would induce a rapid change in their profile. We did not detect changes in the total amount of macrophages in the islets of Abn-CBD- versus vehicle-treated STZ-injected mice; however, the number of intra-islets proinflammatory M1 macrophages, also known as classically

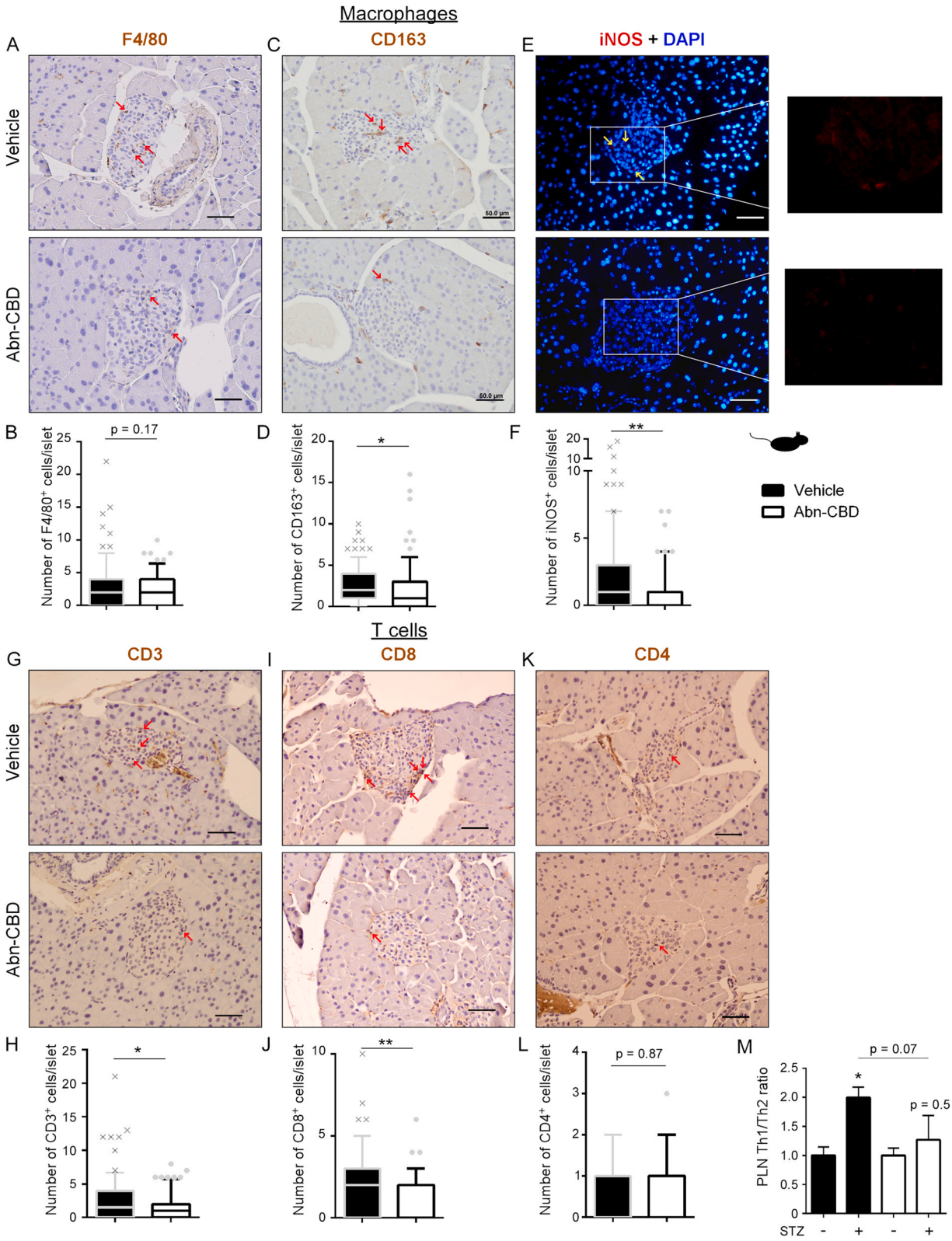

Fig. 6. Analysis of immune cells infiltration in islets of Abn-CBD-treated STZ-induced hyperglycemic mice. Representative images and quantification of pancreas sections immunostained for (A-B) the macrophage marker F4/80, (C-D) the M2 polarized macrophage marker CD163, and (E-F) the M1 polarized macrophage marker iNOS (red staining), and (G-H) the T cell markers CD3, (I-J) CD4 and (K-L) CD8. Sections were counterstained with hematoxylin (A, C, G, I, K) or DAPI (E) to stain the nuclei (blue staining). Data are shown in box & whiskers plot with 10–90 percentile of vehicle- (black bars) and Abn-CBD-treated (white bars) mice. The scale bar is 50 μm. N = 9 mice per group, N = 90–100 islets per group. * $p < 0.05$ and * *$p < 0.01$ compared to vehicle. Non-significant p values are shown compared to vehicle. (M) Ratio of Th1/non-Th1 cells in pancreatic lymph nodes (PLN). Data are mean ± S.E.M. N = 4 mice per group. * $p < 0.05$ compared to control (no STZ). Non-significant p values are shown compared to vehicle.

activated macrophages, were significantly lower in the Abn-CBD-treated mice. IFN-γ induces the polarization of macrophages to M1 [47], which are involved in the Th1 response. Indeed, M1 macrophages secrete pro-inflammatory cytokines such as TNF-α and IL-6 [47], which were decreased in Abn-CBD-treated mice, as well as the Th1/non-Th1 $CD4^+$ ratio, compared to vehicle-treated mice.

We also investigated the molecular mechanisms underlying these anti-inflammatory and anti-apoptotic effects of Abn-CBD in the islets of T1D mice. The NF-κB pathway and the inflammasome are key components in the regulation of inflammation and beta cell survival as, when activated, they synergistically work to promote beta cell death [34,38]. STZ-induced beta cell damage involve elevated TXNIP expression and subsequent activation of the inflammasome [29–31]. At the molecular level, we found that Abn-CBD repressed activation of both NF-κB (measured as phosphorylation of p65) and the inflammasome (measured as TXNIP staining) in islets from NOD and STZ-challenged mice treated with Abn-CBD, which explains a reduced inflammation-mediated beta cell death and fibrosis. Thus, the anti-apoptotic effect of Abn-CBD in beta cells seems to arise from a combination of lower levels of cytokines and chemokines in circulation, decreased inflammation and immune infiltration into the islets, and reduced sensitivity to cytokines by beta cells [18,19,26]. The reduced insulitis concurs with lower $CD4^+$ T cells polarization to Th1, dampening Th1/Th2 ratio, and subsequently decreasing CTL cells maturation and infiltration, and lowering the presence of M1 macrophages in the islets. On the other side, down-regulation of the NF-κB pathway and the inflammasome may be responsible for a reduced beta cell sensitivity to cytokines and reduced islet cytokines secretion, further preventing T cell infiltration.

Limitations of the current study are the short-term treatment and the lack of comparison with human data. A longer treatment of NOD mice would elucidate whether Abn-CBD delays the progression of insulitis sufficiently to lead to a relevant delay on the onset of T1D. Longer treatments and studies using human samples are a justified need.

5. Conclusions

Overall, our work shows that Abn-CBD is a potent modulator of the aberrant inflammatory response characteristic of T1D. At diagnosis, around 50% of patients with T1D go through what is called the honeymoon phase for as long as 1 year, in which the residual beta cells can maintain normoglycemia without the need for exogenous insulin [48]. We herein provide evidence that cannabinoids such as the Abn-CBD modulate the immune response and beta cell death at the early stages of T1D and protect beta cells from stress. Hence, they are promising compounds that merit further clinical development and, if successful, they could be useful for pharmacological interventions aimed at stopping insulitis and beta cell loss at early stages of T1D, especially in patients entering the honeymoon phase of the disease.

Ethics approval statement

Animal care and experimental procedures were approved by the Animal Experimentation Ethics Committee of the Malaga University and authorized by the government of Andalucia, Spain, (Project number 28/06/2018/107). The European directive 2010/63/EU on the use of animals for research purposes was followed as well as the ARRIVE 2.0 guidelines on reporting experiments involving animals or animal tissue.

CRediT authorship contribution statement

Isabel Gonzalez-Mariscal: Conceptualization, Formal analysis, Funding acquisition, Investigation, Methodology, Project administration, Resources, Supervision, Validation, Visualization, Writing – original draft, Writing – review & editing. **Macarena Pozo-Morales:** Formal analysis, Methodology. Silvana Y. Romero-Zerbo: Formal analysis, Methodology. **Vanesa Espinosa-Jimenez:** Formal analysis, Methodology. **Alejandro Escamilla-Sánchez:** Formal analysis, Methodology. **Lourdes Sánchez-Salido:** Formal analysis, Methodology. **Nadia Cobo-Vuilleumier:** Formal analysis. **Benoit R. Gauthier:** Formal analysis, Writing – review & editing. **Francisco J. Bermudez-Silva:** Conceptualization, Funding acquisition, Project administration, Resources, Supervision, Validation, Visualization, Writing – original draft, Writing – review & editing.

Authors contribution

IGM and FJBS conceptualized and supervised the study and obtained funding. IGM, MPM, SYRZ, and VEJ performed in vivo and in vitro experiments. AES AND LSS performed histology, immunohistochemistry and immunofluorescence. IGM, NCV, BRG and FJBS performed formal analysis. IGM and FJBS wrote the manuscript.

Supplementary material

Figure S1. **Effect of STZ and Abn-CBD on islet structure.** Analysis of (A) islet area frequency distribution and (B) mean islet area in citrate buffer-vehicle- (control; white circles, dotted line), STZ-vehicle- (black squares, black bars) and STZ-Abn-CBD-treated mice (grey triangles, white bars). (C) Quantification of islet cell apoptosis and $CD3^+$ T cell infiltration in islets from citrate buffer-vehicle-, STZ-vehicle- and STZ-Abn-CBD-treated mice. Data are mean ± S.E.M. $N = 9$ mice per group, $N = 90–100$ islets per group. * $p < 0.05$, * *$p < 0.01$ and * **$p < 0.001$ compared to STZ-vehicle.

Conflict of interest statement

The authors declare no conflict of interest.

Acknowledgements

Funding: H2020-MSCA-IF-2016, Grant Agreement number: 748749, EU. Consejeria de Salud y Familias, Junta de Andalucia, Spain (PI-0318-2018). Instituto de Salud Carlos III, Ministerio de Sanidad, Gobierno de España, Spain (PI17/01004). Ministerio de Ciencia, Innovación y Universidades, Agencia Estatal de Investigación and Fondo Europeo de Desarrollo Regional, Spain (BFU2017-83588-P to BRG). We thank all the staff of the animal facility at IBIMA (ECAI de Experimentación Animal) and especially its coordinator Dr. Ricardo González Carrascosa for his excellent work. The authors also gratefully acknowledge all the staff of the bioimaging facility at IBIMA (ECAI de Imagen) and the proteomic (ECAI de Proteómica) facility, especially Dra. Carolina Lobo-García for excellent technical assistance. FJBS and IGM belong to the regional "Nicolás Monardes" research program from Consejería de Salud y Familias (C-0070-2012, RC0005-2016, RC-0001-2021 and C1-0018-2019; Junta de Andalucía, Spain). FJBS, NCV and BRG are members of the pancreatic islets study group from the Spanish Society for Diabetes (SED), Spain. CIBERDEM is an initiative of the Instituto de Salud Carlos III, Spain.

Appendix A. Supporting information

Supplementary data associated with this article can be found in the online version at doi:10.1016/j.biopha.2021.112361.

References

[1] International Diabetes Federation, IDF Diabetes Atlas, (n.d.). https://www.idf.org/e-library/epidemiology-research/diabetes-atlas.html (Accessed 15 May 2018).
[2] I.M. Talaat, A. Nasr, A.A. Alsulaimani, H. Alghamdi, K.A. Alswat, D.M. Almalki, A. Abushouk, A.M. Saleh, G. Allam, Association between type 1, type 2 cytokines, diabetic autoantibodies and 25-hydroxyvitamin D in children with type 1 diabetes, J. Endocrinol. Investig. 39 (2016) 1425–1434, https://doi.org/10.1007/s40618-016-0514-9.

[3] K. Alnek, K. Kisand, K. Heilman, A. Peet, K. Varik, R. Uibo, Increased blood levels of growth factors, proinflammatory cytokines, and Th17 cytokines in patients with newly diagnosed type 1 diabetes, PLoS One 10 (2015), e0142976, https://doi.org/10.1371/journal.pone.0142976.

[4] N.G. Forouhi, N.J. Wareham, Epidemiology of diabetes, Medicine 42 (2014) 698–702, https://doi.org/10.1016/j.mpmed.2014.09.007.

[5] C.E.B. Couri, K.C.R. Malmegrim, M.C. Oliveira, New horizons in the treatment of type 1 diabetes: more intense immunosuppression and beta cell replacement, Front. Immunol. 9 (2018) 1086, https://doi.org/10.3389/fimmu.2018.01086.

[6] N. Cobo-Vuilleumier, B.R. Gauthier, Time for a paradigm shift in treating type 1 diabetes mellitus: coupling inflammation to islet regeneration, Metab.: Clin. Exp. 104 (2020), 154137, https://doi.org/10.1016/j.metabol.2020.154137.

[7] I. González-Mariscal, S.M. Krzysik-Walker, M.E. Doyle, Q.-R. Liu, R. Cimbro, S. Santa-Cruz Calvo, S. Ghosh, Ł. Cieśla, R. Moaddel, O.D. Carlson, R.P. Witek, J. F. O'Connell, J.M. Egan, Human CB1 receptor isoforms, present in hepatocytes and β-cells, are involved in regulating metabolism, Sci. Rep. 6 (2016) 33302, https://doi.org/10.1038/srep33302.

[8] S. Engeli, Dysregulation of the endocannabinoid system in obesity, J. Neuroendocrinol. 20 (Suppl 1) (2008) 110–115, https://doi.org/10.1111/j.1365-2826.2008.01683.x.

[9] I. González-Mariscal, S.M. Krzysik-Walker, W. Kim, M. Rouse, J.M. Egan, Blockade of cannabinoid 1 receptor improves GLP-1R mediated insulin secretion in mice, Mol. Cell. Endocrinol. 423 (2016) 1–10, https://doi.org/10.1016/j.mce.2015.12.015.

[10] T. Jourdan, G. Godlewski, R. Cinar, A. Bertola, G. Szanda, J. Liu, J. Tam, T. Han, B. Mukhopadhyay, M.C. Skarulis, C. Ju, M. Aouadi, M.P. Czech, G. Kunos, Activation of the Nlrp3 inflammasome in infiltrating macrophages by endocannabinoids mediates beta cell loss in type 2 diabetes, Nat. Med. 19 (2013) 1132–1140, https://doi.org/10.1038/nm.3265.

[11] I. González-Mariscal, R.A. Montoro, M.E. Doyle, Q.-R. Liu, M. Rouse, J. F. O'Connell, S. Santa-Cruz Calvo, S.M. Krzysik-Walker, S. Ghosh, O.D. Carlson, E. Lehrmann, Y. Zhang, K.G. Becker, C.W. Chia, P. Ghosh, J.M. Egan, Absence of cannabinoid 1 receptor in beta cells protects against high-fat/high-sugar diet-induced beta cell dysfunction and inflammation in murine islets, Diabetologia 61 (2018) 1470–1483, https://doi.org/10.1007/s00125-018-4576-4.

[12] R. Cinar, G. Godlewski, J. Liu, J. Tam, T. Jourdan, B. Mukhopadhyay, J. Harvey-White, G. Kunos, Hepatic cannabinoid-1 receptors mediate diet-induced insulin resistance by increasing de novo synthesis of long-chain ceramides, Hepatology 59 (2014) 143–153, https://doi.org/10.1002/hep.26606.

[13] P. Pacher, N.M. Kogan, R. Mechoulam, Beyond THC and endocannabinoids, Annu. Rev. Pharmacol. Toxicol. 60 (2020) 637–659, https://doi.org/10.1146/annurev-pharmtox-010818-021441.

[14] L. Weiss, M. Zeira, S. Reich, S. Slavin, I. Raz, R. Mechoulam, R. Gallily, Cannabidiol arrests onset of autoimmune diabetes in NOD mice, Neuropharmacology 54 (2008) 244–249, https://doi.org/10.1016/j.neuropharm.2007.06.029.

[15] M.D. Adams, J.T. Earnhardt, B.R. Martin, L.S. Harris, W.L. Dewey, R.K. Razdan, A cannabinoid with cardiovascular activity but no overt behavioral effects, Experientia 33 (1977) 1204–1205, https://doi.org/10.1007/bf01922330.

[16] A. Tomko, L. O'Leary, H. Trask, J.C. Achenbach, S.R. Hall, K.B. Goralski, L.D. Ellis, D.J. Dupré, Antitumor activity of abnormal cannabidiol and its analog O-1602 in taxol-resistant preclinical models of breast cancer, Front. Pharmacol. 10 (2019) 1124, https://doi.org/10.3389/fphar.2019.01124.

[17] A.M. McKillop, B.M. Moran, Y.H.A. Abdel-Wahab, P.R. Flatt, Evaluation of the insulin releasing and antihyperglycaemic activities of GPR55 lipid agonists using clonal beta-cells, isolated pancreatic islets and mice, Br. J. Pharmacol. 170 (2013) 978–990, https://doi.org/10.1111/bph.12356.

[18] I. Ruz-Maldonado, A. Pingitore, B. Liu, P. Atanes, G.C. Huang, D. Baker, F. J. Alonso, F.J. Bermúdez-Silva, S.J. Persaud, LH-21 and abnormal cannabidiol improve β-cell function in isolated human and mouse islets through GPR55-dependent and -independent signalling, Diabetes, Obes. Metab. 20 (2018) 930–942, https://doi.org/10.1111/dom.13180.

[19] C.T. Vong, H.H.L. Tseng, Y.W. Kwan, S.M.-Y. Lee, M.P.M. Hoi, Novel protective effect of O-1602 and abnormal cannabidiol, GPR55 agonists, on ER stress-induced apoptosis in pancreatic β-cells, Biomed. Pharmacother. 111 (2019) 1176–1186, https://doi.org/10.1016/J.BIOPHA.2018.12.126.

[20] C.T. Vong, H.H.L. Tseng, Y.W. Kwan, S.M.-Y. Lee, M.P.M. Hoi, G-protein coupled receptor 55 agonists increase insulin secretion through inositol trisphosphate-mediated calcium release in pancreatic β-cells, Eur. J. Pharmacol. 854 (2019) 372–379, https://doi.org/10.1016/j.ejphar.2019.04.050.

[21] I. Ruz-Maldonado, A. Pingitore, B. Liu, P. Atanes, G.C. Huang, D. Baker, F. J. Alonso, F.J. Bermúdez-Silva, S.J. Persaud, LH-21 and abnormal cannabidiol improve β-cell function in isolated human and mouse islets through GPR55-dependent and -independent signalling, Diabetes Obes. Metab. 20 (2018) 930–942, https://doi.org/10.1111/dom.13180.

[22] D. Yin, J. Tao, D.D. Lee, J. Shen, M. Hara, J. Lopez, A. Kuznetsov, L.H. Philipson, A. S. Chong, Recovery of islet β-cell function in streptozotocin-induced diabetic mice: an indirect role for the spleen, Diabetes 55 (2006) 3256–3263, https://doi.org/10.2337/db05-1275.

[23] S.Y. Romero-Zerbo, I. Ruz-Maldonado, V. Espinosa-Jiménez, A. Rafacho, A. I. Gómez-Conde, L. Sánchez-Salido, N. Cobo-Vuilleumier, B.R. Gauthier, F. J. Tinahones, S.J. Persaud, F.J. Bermúdez-Silva, The cannabinoid ligand LH-21 reduces anxiety and improves glucose handling in diet-induced obese pre-diabetic mice, Sci. Rep. 7 (2017) 3946, https://doi.org/10.1038/s41598-017-03292-w.

[24] M.C. Gagnerault, J.J. Luan, C. Lotton, F. Lepault, Pancreatic lymph nodes are required for priming of β cell reactive T cells in NOD mice, J. Exp. Med. 196 (2002) 369–377, https://doi.org/10.1084/jem.20011353.

[25] N. Cobo-Vuilleumier, P.I. Lorenzo, N.G. Rodríguez, I. de, G. Herrera Gómez, E. Fuente-Martin, L. López-Noriega, J.M. Mellado-Gil, S.-Y. Romero-Zerbo, M. Baquié, C.C. Lachaud, K. Stifter, G. Perdomo, M. Bugliani, V. De Tata, D. Bosco, G. Parnaud, D. Pozo, A. Hmadcha, J.P. Florido, M.G. Toscano, P. de Haan, K. Schoonjans, L. Sánchez Palazón, P. Marchetti, R. Schirmbeck, A. Martín-Montalvo, P. Meda, B. Soria, F.-J. Bermúdez-Silva, L. St-Onge, B.R. Gauthier, LRH-1 agonism favours an immune-islet dialogue which protects against diabetes mellitus, Nat. Commun. 9 (2018) 1488, https://doi.org/10.1038/s41467-018-03943-0.

[26] S.Y. Romero-Zerbo, M. García-Fernández, V. Espinosa-Jiménez, M. Pozo-Morales, A. Escamilla-Sánchez, L. Sánchez-Salido, E. Lara, N. Cobo-Vuilleumier, A. Rafacho, G. Olveira, G. Rojo-Martínez, B.R. Gauthier, I. González-Mariscal, F.J. Bermúdez-Silva, The atypical cannabinoid abn-CBD reduces inflammation and protects liver, pancreas, and adipose tissue in a mouse model of prediabetes and non-alcoholic fatty liver disease, Front. Endocrinol. 11 (2020) 103, https://doi.org/10.3389/fendo.2020.00103.

[27] A.M. McKillop, B.M. Moran, Y.H.A. Abdel-Wahab, N.M. Gormley, P.R. Flatt, Metabolic effects of orally administered small-molecule agonists of GPR55 and GPR119 in multiple low-dose streptozotocin-induced diabetic and incretin-receptor-knockout mice, Diabetologia 59 (2016) 2674–2685, https://doi.org/10.1007/s00125-016-4108-z.

[28] M.A. Atkinson, Evaluating preclinical efficacy, Sci. Transl. Med. 3 (2011) 96, https://doi.org/10.1126/scitranslmed.3002757.

[29] Z.T. Kelleher, Y. Sha, M.W. Foster, W.M. Foster, M.T. Forrester, H.E. Marshall, Thioredoxin-mediated denitrosylation regulates cytokine-induced nuclear factor κB (NF-κB) activation, J. Biol. Chem. 289 (2014) 3066–3072, https://doi.org/10.1074/jbc.M113.503938.

[30] R. Zhou, A. Tardivel, B. Thorens, I. Choi, J. Tschopp, Thioredoxin-interacting protein links oxidative stress to inflammasome activation, Nat. Immunol. 11 (2010) 136–140, https://doi.org/10.1038/ni.1831.

[31] K. Maedler, P. Sergeev, F. Ris, J. Oberholzer, H.I. Joller-Jemelka, G.A. Spinas, N. Kaiser, P.A. Halban, M.Y. Donath, R. Unger, S. Grundy, N. Kaiser, A. Corcos, I. Sarel, E. Cerasi, J. Leahy, H. Cooper, D. Deal, G. Weir, R. Robertson, L. Rossetti, A. Giaccari, R. DeFronzo, D. Eizirik, G. Korbutt, C. Hellerstrom, S. Marshak, M. Donath, D. Gross, E. Cerasi, N. Kaiser, K. Maedler, M. Federici, I. Efanova, K. Maedler, Y. Tajiri, C. Moller, V. Grill, R. Robertson, H. Zhang, K. Pyzdrowski, T. Walseth, R. Robertson, L. Olson, H. Zhang, T. Mandrup-Poulsen, T. Mandrup-Poulsen, K. Bendtzen, J. Nielsen, G. Bendixen, J. Nerup, K. Bendtzen, G. Spinas, T. Mandrup-Poulsen, G. Spinas, K. Yamada, J. Corbett, J. Lancaster, M. Sweetland, M. McDaniel, N. Giannoukakis, N. Giannoukakis, A. Loweth, G. Williams, R. James, J. Scarpello, N. Morgan, A. Rabinovitch, W. Sumoski, R. Rajotte, G. Warnock, G. Stassi, G. Kwon, J. Corbett, C. Rodi, P. Sullivan, M. McDaniel, M. Darville, D. Eizirik, M. Flodstrom, N. Welsh, D. Eizirik, E. Linetsky, J. Oberholzer, C. Ricordi, P. Lacy, E. Finke, B. Olack, D. Scharp, N. Kaiser, A. Corcos, I. Sarel, E. Cerasi, S. Jodo, M. Schneemann, Y. Gavrieli, Y. Sherman, S. Ben-Sasson, M. Karin, D. Mathis, L. Vence, C. Benoist, M. Pietropaolo, E. Barinas-Mitchell, S. Pietropaolo, L. Kuller, M. Trucco, M. Rowley, I. Mackay, Q. Chen, W. Knowles, P. Zimmet, T. Wilkin, M. Bellone, J. Trudeau, P. Lacy, E. Finke, P. Lacy, M. Arnush, A. Scarim, M. Heitmeier, C. Kelly, J. Corbett, M. Heitmeier, M. Arnush, A. Scarim, J. Corbett, M. Gadot, M. Chen, P. Proost, C. Gysemans, C. Mathieu, D. Eizirik, D. Eizirik, M. Darville, D. Liu, U. Zumsteg, S. Frigerio, G. Hollander, N. Giannoukakis, W. Rudert, M. Trucco, P. Robbins, J. Corbett, M. Sweetland, J. Wang, J. Lancaster, M. McDaniel, H. Heimberg, Glucose-induced beta cell production of IL-1beta contributes to glucotoxicity in human pancreatic islets, J. Clin. Investig. 110 (2002) 851–860, https://doi.org/10.1172/JCI15318.

[32] A.H. Minn, C. Hafele, A. Shalev, Thioredoxin-interacting protein is stimulated by glucose through a carbohydrate response element and induces β-cell apoptosis, Endocrinology 146 (2005) 2397–2405, https://doi.org/10.1210/en.2004-1378.

[33] Z.T. Kelleher, Y. Sha, M.W. Foster, W.M. Foster, M.T. Forrester, H.E. Marshall, Thioredoxin-mediated denitrosylation regulates cytokine-induced nuclear factor κB (NF-κB) activation, J. Biol. Chem. 289 (2014) 3066–3072, https://doi.org/10.1074/jbc.M113.503938.

[34] R. Zhou, A. Tardivel, B. Thorens, I. Choi, J. Tschopp, Thioredoxin-interacting protein links oxidative stress to inflammasome activation, Nat. Immunol. 11 (2010) 136–140, https://doi.org/10.1038/ni.1831.

[35] K.J. Hunt, N.L. Baker, P.A. Cleary, R. Klein, G. Virella, M.F. Lopes-Virella, Longitudinal association between endothelial dysfunction, inflammation, and clotting biomarkers with subclinical atherosclerosis in type 1 diabetes: an evaluation of the DCCT/EDIC cohort, Diabetes Care 38 (2015) 1281–1289, https://doi.org/10.2337/dc14-2877.

[36] C.O. Eleazu, K.C. Eleazu, S. Chukwuma, U.N. Essien, Review of the mechanism of cell death resulting from streptozotocin challenge in experimental animals, its practical use and potential risk to humans, J. Diabetes Metab. Disord. 12 (2013) 60, https://doi.org/10.1186/2251-6581-12-60.

[37] I. González-Mariscal, B. Carmona-Hidalgo, M. Winkler, J.D. Unciti-Broceta, A. Escamilla, M. Gómez-Cañas, J. Fernández-Ruiz, B.L. Fiebich, S.-Y. Romero-Zerbo, F.J. Bermúdez-Silva, J.A. Collado, E. Muñoz, (+)-Trans-cannabidiol-2-hydroxy pentyl is a dual CB1R antagonist/CB2R agonist that prevents diabetic nephropathy in mice, Pharmacol. Res. 169 (2021), 105492, https://doi.org/10.1016/j.phrs.2021.105492.

[38] C.M. Artlett, J.D. Thacker, Molecular activation of the NLRP3 inflammasome in fibrosis: common threads linking divergent fibrogenic diseases, Antioxid. Redox Signal. 22 (2015) 1162–1175, https://doi.org/10.1089/ars.2014.6148.

[39] E. Kuric, P. Seiron, L. Krogvold, B. Edwin, T. Buanes, K.F. Hanssen, O. Skog, K. Dahl-Jørgensen, O. Korsgren, Demonstration of tissue resident memory CD8 T

cells in insulitic lesions in adult patients with recent-onset type 1 diabetes, Am. J. Pathol. 187 (2017) 581–588, https://doi.org/10.1016/j.ajpath.2016.11.002.
[40] B. Devendra, J. Jasinski, E. Melanitou, M. Nakayama, M. Li, B. Hensley, J. Paronen, H. Moriyama, D. Miao, G.S. Eisenbarth, E. Liu, Interferon-α as a mediator of polyinosinic:polycytidylic acid-induced type 1 diabetes, Diabetes 54 (2005) 2549–2556, https://doi.org/10.2337/diabetes.54.9.2549.
[41] Y. Zhang, B. O'Brien, J. Trudeau, R. Tan, P. Santamaria, J.P. Dutz, In situ β cell death promotes priming of diabetogenic CD8 T lymphocytes, J. Immunol. 168 (2002) 1466–1472, https://doi.org/10.4049/jimmunol.168.3.1466.
[42] T. Tomita, Immunocytochemical localization of cleaved caspase-3 in pancreatic islets from type 1 diabetic subjects, Islets 2 (2010) 24–29, https://doi.org/10.4161/isl.2.1.10041.
[43] C. Hundhausen, A. Roth, E. Whalen, J. Chen, A. Schneider, S.A. Long, S. Wei, R. Rawlings, M. Kinsman, S.P. Evanko, T.N. Wight, C.J. Greenbaum, K. Cerosaletti, J.H. Buckner, Enhanced T cell responses to IL-6 in type 1 diabetes are associated with early clinical disease and increased IL-6 receptor expression, Sci. Transl. Med. 8 (2016) 356ra119, https://doi.org/10.1126/scitranslmed.aad9943.
[44] K. Alnek, K. Kisand, K. Heilman, A. Peet, K. Varik, R. Uibo, Increased blood levels of growth factors, proinflammatory cytokines, and Th17 cytokines in patients with newly diagnosed type 1 diabetes, PLoS One 10 (2015), e0142976, https://doi.org/10.1371/journal.pone.0142976.
[45] S. Lindley, C.M. Dayan, A. Bishop, B.O. Roep, M. Peakman, T.I.M. Tree, Defective suppressor function in CD4+CD25+ T-cells from patients with type 1 diabetes, Diabetes 54 (2005) 92–99, https://doi.org/10.2337/diabetes.54.1.92.
[46] T. Brusko, C. Wasserfall, K. McGrail, R. Schatz, H.L. Viener, D. Schatz, M. Haller, J. Rockell, P. Gottlieb, M. Clare-Salzler, M. Atkinson, No alterations in the frequency of FOXP3+ regulatory T-cells in type 1 diabetes, Diabetes 56 (2007) 604–612, https://doi.org/10.2337/db06-1248.
[47] Y. Yao, X.H. Xu, L. Jin, Macrophage polarization in physiological and pathological pregnancy, Front. Immunol. 10 (2019), https://doi.org/10.3389/fimmu.2019.00792.
[48] V. Katchan, P. David, Y. Shoenfeld, Cannabinoids and autoimmune diseases: a systematic review, Autoimmun. Rev. 15 (2016) 513–528, https://doi.org/10.1016/J.AUTREV.2016.02.008.